GEOPHYSICAL RESEARCH LETTERS, VOL. 25, NO. 20, PAGES 3747-3750, OCTOBER 15, 1998

A new auroral feature: The nightside gap

D. Chua,[1] M. Brittnacher,[1] G. Parks,[1] G. Germany,[2] and J. Spann[3]

Abstract. Using images from the Ultraviolet Imager (UVI) aboard the Polar spacecraft, we identify an unusual morphological feature of the auroral oval marked by roughly a factor of four decrease in auroral luminosity near local midnight during some substorms. This feature has not been previously described in detail. The nightside gap appears in roughly 7% of the substorms observed by UVI during our study period from December, 1996 to February, 1997. Two nightside gap events from this period are characterized in detail as case studies of this phenomenon. We suggest that the nightside gap may be due to a significant reduction in field-aligned currents along with an insufficient ionospheric potential to accelerate precipitating electrons within the gap region, perhaps associated with the Harang discontinuity.

Introduction

Global images of the nightside auroral oval commonly show contiguous regions of precipitation during substorm activity. However, observations by the Ultraviolet Imager (UVI) on board the Polar spacecraft demonstrate a well defined discontinuity in the nightside auroral oval during some substorm periods. Although *Elphinstone* [1995] and *Lui et al.* [1995] have described structures in the auroral oval separated by gaps, such as spatially periodic auroral beads, the nightside gap represents a much more extended region of reduced luminosity across approximately 1.0 hour in local time near midnight. While the midday gap that occurs near local noon has been previously studied [*Dandekar and Pike*, 1978], this gap in the nightside oval has been a largely undiscussed feature. *Lui et al.* [1995] describe a relative void of auroral emissions near local midnight during a substorm on July 24, 1986 and conjectured that this phenomenon may have been associated with a sharp, northward turning of the interplanetary magnetic field (IMF) during high solar wind dynamic pressure. In this preliminary report we characterize the average properties of the nightside gap and present two events that occur on January 18, 1997 and January 23, 1997 as case studies.

Observations

The UVI instrument [*Torr et al.*, 1995] provides global imaging of the aurora borealis over periods of several hours with a time resolution on the order of minutes. The images presented in this report (Figure 1) are taken from an altitude near 8 R_E, where the UVI instrument has a spatial resolution of 40 × 35 km pixel^{-1}. Images of the auroral oval are shown in the Apex magnetic coordinate system [*Richmond*, 1995], with the color scale denoting the energy flux (erg cm^{-2} s^{-1}) determined from each 37-second exposure through the Lyman-Birge-Hopfield band, short (LBHs: 140-160 nm) and long (LBHl: 160-180 nm) wavelength filters [e.g., *Brittnacher et al.*, 1997]. We define the boundaries of the nightside gap to be where the mean energy flux on either side of the gap falls by a factor of four. For all event periods in this study, solar wind plasma parameters are provided by the SWE instrument [*Ogilvie et al.*, 1995] and IMF measurements are given by the MFI experiment [*Lepping et al.*, 1995], both on the Wind spacecraft.

January 18, 1997

The gap occuring in the nightside oval on January 18, 1997 appears when precipitation commences across both pre-midnight and early dawn sectors at approximately 02:04 UT while the region around local midnight remains inactive (Figure 1a). The gap region is roughly centered around local midnight between 2330 MLT and 0050 MLT, spanning 1.3 ± 0.3 hours in local time (930 ± 215 km), and extending across the entire north-south dimension of the auroral oval. Since the regions of auroral emission surrounding the gap show no substantial poleward motion during the 8 minutes that the discontinuity is observed (02:04-02:12 UT), we determine that this activity is brightening of the oval prior to substorm onset rather than localized breakups. A wobble present in the Polar spacecraft's motion causes a 1×10 pixel smearing in the images shown here. However, during this period the wobble is roughly along the north-south dimension of the gap and does not significantly affect the east-west distribution of auroral luminosity across the discontinuity in the midnight sector. The primary effect is to exaggerate the equatorward and poleward boundaries of the oval as can be seen in Figure 1.

Between 02:04-02:12 UT (Figure 1a), the average energy fluxes in the auroral oval measured 15 minutes in

[1]Geophysics Program, University of Washington, Seattle, WA

[2]Center for Space Plasma and Aeronomic Research, University of Alabama in Huntsville, Huntsville, AL.

[3]NASA Marshall Space Flight Center, Hunstville, AL

Paper number 98GL02806.
0094-8276/98/98GL-02806$05.00

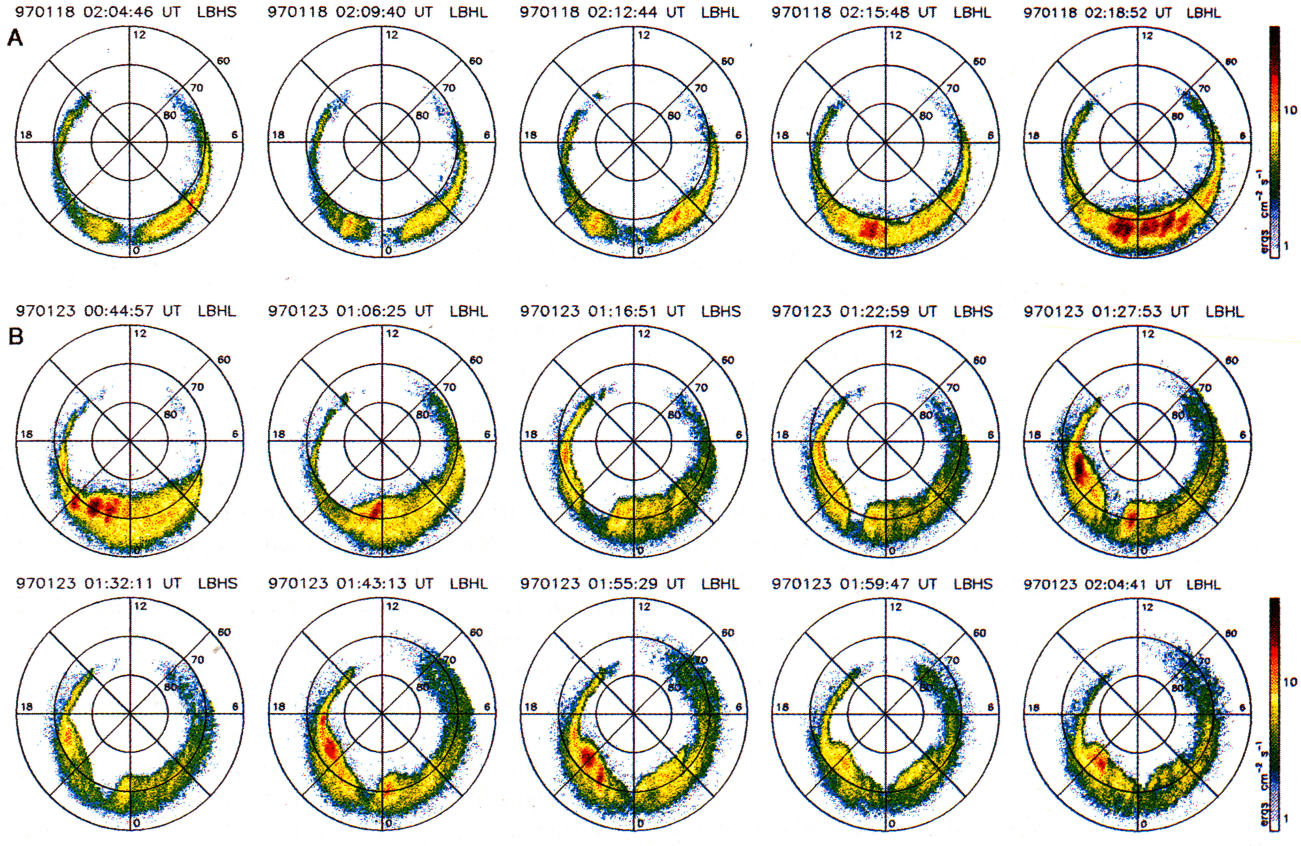

Figure 1. UVI images for (A) January 18, 1997 and (B) January 23, 1997. The color bar is scaled logarithmically in units of erg cm^{-2} s^{-1} . The wobble signature has not been removed from these images (See text).

local time (~ 190 km) away from the duskward and dawnward edges of the gap are 5.0 erg cm^{-2} s^{-1} and 6.7 erg cm^{-2} s^{-1}, respectively. In comparison, the average energy flux at the centroid of gap is only 1.5 erg cm^{-2} s^{-1}, or about 25% of that in the surrounding nightside oval. The energy flux within the gap is still, however, well above the minimum detectable energy flux of 0.2 erg cm^{-2} s^{-1}, corresponding to the one count level in the UVI camera. The discontinuity is terminated by a sudden and dramatic increase in precipitation across the gap region after 02:12 UT, with a substorm onset in the 2300-2400 MLT sector filling in the gap at roughly 02:15 UT. As a result, the energy flux in the region where the gap had been rises by an order of magnitude to values between 10.0-17.0 erg cm^{-2} s^{-1}.

In order to match the IMF observations at the Wind spacecraft location with the features in the UVI images, we estimate a propogation correction of 30 minutes based on a solar wind velocity of roughly 330 km s^{-1} (Figure 2). Over the course of the event, IMF B_z is increasing northward from roughly -5 nT to -1 nT, with the substorm onset in the gap region between 02:15-02:18 UT (Figure 1a) occuring close to the time when B_z reaches its least negative value. The B_y component shows a negative turning from 2.5 nT to roughly -5 nT near 01:35 UT at the Wind location, or 02:05 UT at the magnetopause, approximately the time of the gap appearance. Solar wind dynamic pressure is steady at levels near 3 nPa during this event (Figure 2).

January 23, 1997

The nightside gap observed on January 23, 1997 occurs during a multiple onset event, making the relation of this gap to substorm phase uncertain. The gap is first evident in the 01:16 UT image (Figure 1b) as the region of inactivity surrounded on the dawnward side by the remnants of the previous poleward expansion shown between 00:44-01:06 UT and an intensification commencing in the dusk sector (1800-2100 MLT). At

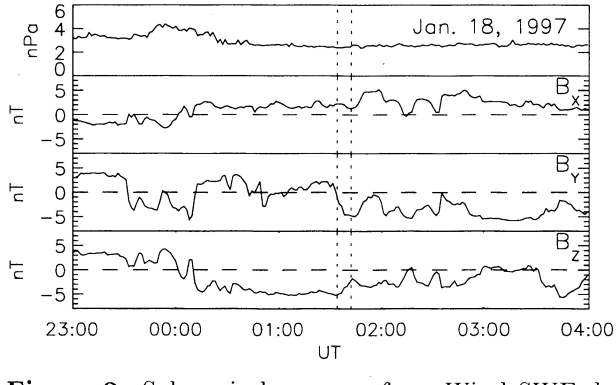

Figure 2. Solar wind pressure from Wind SWE data [*Ogilvie et al.*, 1995] and IMF data from the Wind MFI experiment [*Lepping et al.*, 1995] during the January 18, 1997 gap, shown at the Wind spacecraft location in GSM coordinates. The times corresponding to the gap event are marked by the vertical dotted lines, taking into account an estimated propagation correction of 30 minutes.

01:16 UT, the duskward and dawnward boundaries of the gap lie at approximately 2235 MLT and 2340 MLT, with an average width over the event of 1.1 ± 0.3 MLT hours (790 ± 215 km). As with the January 18 images, the spacecraft wobble has minimal effect on the longitudinal distribution of auroral luminosity near the nightside gap. Although the gap appears to shift dawnward between the 01:16 UT and 01:55 UT images, this is more likely due to poleward expansion in the dusk sector and the recession of the auroral oval region on the dawn side of the gap. In contrast to the previous example, the January 23, 1997 event persists for roughly 45 minutes and does not quickly progress into a substorm onset within the gap. Rather, the gap boundaries become increasingly ambiguous after the 01:59 UT image as the oval becomes more quiescent.

As with the previous example, we find sharp gradients in energy flux across the boundaries of the nightside gap. The energy flux at the gap centroid averaged between 01:16 UT and 01:32 UT is 1.6 erg cm^{-2} s^{-1}, with energy fluxes 15 minutes in MLT (~ 190 km) away from the gap exceeding 7.0 erg cm^{-2} s^{-1}. Latitudinal variations in energy flux within the gap region are also seen during this event as shown between 01:16 UT and 01:32 UT. Energy flux near the equatorward region of the gap is measured between 2.0-2.6 erg cm^{-2} s^{-1}, while poleward, it is lower by a factor of two.

The IMF components at the Wind spacecraft position during the January 23 event are shown in Figure 3. A propagation correction of 48 minutes is estimated from a solar wind velocity of approximately 360 km s^{-1} during this time frame. The IMF B_z component had been pointing southward for approximately 1.5 hours, beginning at 23:00 UT (approximately 23:48 UT at the magnetopause), prior to the appearance of the gap near 01:12 UT. Near 00:45 UT at the Wind spacecraft, the IMF B_y exhibits a negative turning and the B_z component increases northward from roughly -3 nT To -1 nT. This feature was also seen in the January 18 event (Figure 2) and is consistent with the observations of *Lui et al.* [1995]. A sector crossing of the IMF B_x and B_y components is observed near 01:00 UT at the Wind spacecraft, with both B_x and B_y turning positive

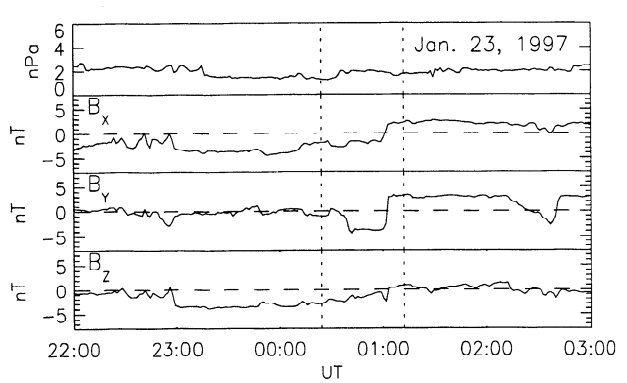

Figure 3. Same as Figure 2 except for the January 23, 1997 event. The estimated IMF propagation correction during this period is estimated at 48 minutes.

and B_z becoming decreasingly southward from -4 nT to approximately 0 nT. The solar wind dynamic pressure during this period is relatively low and steady at approximately 2 nPa (Figure 3).

Discussion

Twenty-two nightside gap events are identified out of 299 substorms (7%) observed in UVI images between December, 1996 and February, 1997. We find that the nightside gap was observed most frequently in the local time sector 2300-0030 MLT, with an average centroid location of 2335 ± 0105 MLT (Figure 4e). The widths of the nightside gaps were fairly evenly distributed between 0.5-1.5 MLT hours, with a mean width of 1.02 ± 0.35 MLT hours, or approximately 730 ± 250 km (Figure 4f). The changes in the IMF B_z and B_y components are estimated between the appearance of the gap and twenty minutes prior, ignoring any sharp variations on the order of a few minutes, for each event in which the Wind spacecraft was in the solar wind (Figures 4c, 4d). A systematic modulation of the MLT location of the gaps and gap width by either ΔB_z or ΔB_y is not evident from our relatively small ensemble of twenty-two events. Moreover, any dependence of gap location or width on the solar wind pressure is not clear.

We have considered whether the nightside gap is an

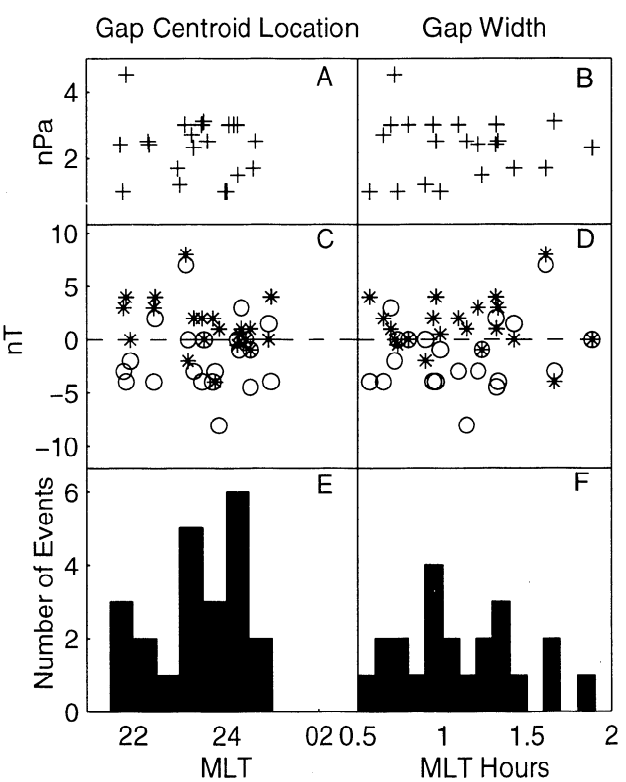

Figure 4. (A) Solar wind pressure versus gap centroid MLT location. (B) Solar wind pressure versus gap MLT width. (C) IMF ΔB_y (open circles) and ΔB_z (asterisks) versus gap centroid MLT location. (D) IMF ΔB_y (open circles) and ΔB_z (asterisks) versus gap MLT width. (E) Distribution of gap centroid location in MLT. (F) Distribution of gap widths in MLT hours.

artifact of the higher energy part of the electron distribution producing emissions in the gap region that we do not observe, but the characteristics of the LBHl filter lead us to conclude that it is a real feature and not an instrumental effect. Because the LBHl filter was designed to pass only those emissions that have no significant losses from O_2 absorption [*Torr et al.*, 1995], the LBHl images register all auroral emissions in that passband regardless of the energy of the incident electrons. The intensity of FUV auroral emissions in the LBHs passband, however, decreases for increasing electron energy, due to O_2 absorption in the lower thermosphere [*Germany et al.*, 1990]. Since the LBII auroral emissions that the UVI observes are due to electron precipitation only, the possibility of other auroral activity within the gap region, due to proton precipitation for example, cannot be discounted. The nightside gap may be spanned by narrow, discrete auroral arcs that we do not resolve due to the spatial resolution of the images near apogee and/or the wobble effect described above. Whatever structure there may be within the gap region, however, is insubstantial relative to the amount of activity just outside the discontinuity.

Kamide and Rostoker [1977] showed that discrete auroral structures are associated with upward field-aligned currents. Assuming that there are few discrete structures in the nightside gap, a likely cause of the drastic decrease in electron precipitation in the discontinuity is a significant reduction of field-aligned currents in that region. This also implies an insufficient ionospheric potential in the gap region to accelerate electrons that give rise to upward field-aligned currents. This reduction in field-aligned currents must be abrupt across local times, and must occur with a characteristic time on the order of tens of minutes, the typical duration of a gap event. *Kunkel et al.* [1986] have shown observations that field-aligned currents can be reduced at or near the Harang discontinuity, the separation between positive and negative disturbances in the horizontal magnetic field component [*Harang*, 1946] which typically occurs in the same local time sector as the nightside gap (2200-2400 MLT). *Kamide* [1978] has even considered the extreme case of having no upward field-aligned currents in that region.

The observations of auroral breakups within the nightside gap region conform with some magnetosphere, ionosphere coupling models [*Kan*, 1993] which suggest substorm expansion to be associated with an instability in the current systems near the Harang discontinuity. *Koskinen and Pulkkinen* [1995] have considered a scenario in which there is no flow of ionospheric plasma across the Harang discontinuity, with Pedersen currents closing through intense, upward field-aligned currents in that region. Our observations would require that these field-aligned currents grow rapidly on time scales of a few minutes, in order to explain the rapid development of substorm onsets within the gap region. The development of a plasma instability associated with this rapid growth of upward field-aligned currents within the gap region may provide a trigger mechanism for the substorms observed to initiate within the discontinuity as shown for January 18, 1997.

Acknowledgments. The authors would like to thank Ryan Wellman, Richard Campell, and Hassan Dougani for their computer support. The research at the University of Washington is supported in part by a NASA grant, NAG5-3170.

References

Brittnacher, M., R. Elsen, G. Parks, L. Chen, G. Germany, and J. Spann, A dayside auroral energy deposition case study using the Polar Ultraviolet Imager, *Geophys. Res. Lett.*, *24*, 991, 1997.

Dandekar, B. S. and C. P. Pike, The midday, discrete auroral gap, *J. Geophys. Res.*, *83*, 4227, 1978.

Elphinstone, R. D. et al., Observations in the vicinity of substorm onset: implications for the substorm process, *J. Geophys. Res.*, *100*, 7937, 1995.

Germany, G. A., M. R. Torr, P. G. Richards, and D. G. Torr, The dependence of modeled OI 1356 and N_2 Lyman Birge Hopfield auroral emissions on the neutral atmosphere, *J. Geophys. Res.*, *95*, 7725, 1990.

Harang, L., The mean field of disturbance of polar geomagnetic storms, *Terr. Mag. Atmos. Electr.*, *51*, 353, 1946.

Kamide, Y., and G. Rostoker, The spatial relationship of field-aligned currents and auroral electrojets to the distribution of nightside auroras, *J. Geophys. Res.*, *82*, 5589, 1977.

Kamide, Y., On current continuity at the Harang discontinuity, *Planet. Spa. Sci.*, *26*, 237, 1978.

Kan, J. R., A global magnetosphere-ionosphere coupling model of substorms, *J. Geophys. Res.*, *98*, 17263, 1993.

Koskinen, H. E. and T. I. Pulkkinen, Midnight velocity shear zone and the concept of Harang discontinuity, *J. Geophys. Res.*, *100*, 9539, 1995.

Kunkel, T., W. Baumjohann, J. Untiedt, and R. A. Greenwald, Electric field and currents at the Harang discontinuity, *J. Geophys.*, *59*, 73, 1986.

Lepping, R. P., et al., The Wind magnetic field investigation, *Space Sci. Rev.*, *71*, 207, 1995.

Lui, A. T. Y., et al., Special features of a substorm during high solar wind dynamic pressure, *J. Geophys. Res.*, *100*, 19095, 1995.

Ogilvie, K. W., et al., SWE, a comprehensive plasma instrument for the Wind spacecraft, *Space Sci. Rev.*, *71*, 55, 1995.

Richmond, A. D., Ionospheric electrodynamics using magnetic apex coordinates, *J. Geomag. Geoelectr.*, *47*, 191, 1995

Torr, M., et al., A far ultraviolet imager for the International Solar-Terrestrial Physics mission, *Space Sci. Rev.*, *71*, 329, 1995.

D. Chua, M. Brittnacher, G. Parks, Geophysics Program, Box 351650, University of Washington, Seattle, WA 98195 (E-mail: damien@gcophys.washington.edu)

G. Germany, CSPAR, University of Alabama in Huntsville, Huntsville, AL 35899

J. Spann, Space Sciences Laboratory, NASA Marshall Space Flight Center, Huntsville, AL 35812

(Received May 8, 1998; revised July 25, 1998; accepted August 5, 1998.)